# LSD1-mediated repression of *GFI1* super-enhancer plays an essential role in erythroleukemia

Goichi Tatsumi[1,2], Masahiro Kawahara[2]*, Ryusuke Yamamoto[1], Masakatsu Hishizawa[1], Katsuyuki Kito[2], Takayoshi Suzuki[3,4], Akifumi Takaori-Kondo[1] and Akira Andoh[2]

**Affiliations**

[1] Department of Hematology and Oncology, Graduate School of Medicine, Kyoto University.

[2] Department of Medicine, Shiga University of Medical Science.

[3] The Institute of Scientific and Industrial Research, Osaka University.

[4] CREST, Japan Science and Technology Agency (JST)

**Contact information**

*Corresponding author: Masahiro Kawahara

E-mail: mkawahar@belle.shiga-med.ac.jp

Address: Seta-Tsukinowa, Otsu, Shiga, 520-2192, Japan

Tel: +81-77-548-2217

Fax: +81-77-548-2219

**Running title:** *GFI1* super-enhancer repression by LSD1 in leukemia

**Supplementary Information**

includes

**Supplementary Materials and Methods**

**Supplementary Figures 1-13**

**Supplementary Tables 1-3**

## Supplementary materials and methods

### Cells

THP-1 cells and murine erythroleukemia cells (MEL) were cultured in RPMI 1640 medium supplemented with 10% fetal bovine serum (FBS) and 1% penicillin. MDS-L cells[1] were cultured in the same medium with 20 ng/ml human interleukin-3 (PeproTech, Rocky Hill, NJ) and 20 μM 2-mercaptoethanol.

### Quantitative PCR

RNA was extracted using either TRIzol reagent (Life Technologies, Carlsbad, CA). Complementary RNA was synthesized by Superscript 3 reverse transcriptase (Thermo Fisher Scientific, Waltham, MA). Quantitative PCR was performed using LightCycler480 System II (Roche, Basel, Switzerland) and a THUNDERBIRD SYBR qPCR mix (Toyobo, Osaka, Japan). Absolute numbers were calculated using the recombinant DNA of targeted amplicons for the standard curve. The primer sequences are provided in Supplementary Table 1.

### Western blotting

Total cell lysates were extracted in lysis buffer [50 mM Tris-HCl at pH 8.0, 150 mM NaCl,

1% Triton X, 1 mM PMSF, 1 mM EDTA, and protease inhibitor cocktail (Nacalai Tesque, Kyoto, Japan)]. We used primary antibodies anti-LSD1 (C69G12, Cell Signaling Technology, Tokyo, Japan) and anti-ACTIN (sc-1616, Santa Cruz Biotechnology, Dallas, TX). HRP-conjugated anti-rabbit (NA934v, GE Healthcare, Little Chalfont, UK) or anti-goat (sc-2020, Santa Cruz Biotechnology) were used as secondary antibodies.

**Cell surface marker assay**

For cell surface marker analysis, murine erythroleukemia cells were stained with anti-Ly6G(Gr-1)-PE-Cy7 (1A8; BD Biosciences, San Jose, CA), and human leukemia cells were stained with anti-CD11b-PE-Cy5 (ICRF44; eBioscience, San Diego, CA) and anti-CD235a-PE-Cy5 (GA-R2; BD Biosciences), and then analyzed by FACS Calibur or CantoII (BD Biosciences).

**Cytology**

Twenty-thousand cells were suspended in phosphate-buffered saline and attached to glass slides by centrifugation at 800 rpm for 4 minutes using Cytospin 4 (Thermo Fisher Scientific). The glass slides were stained with a traditional Wright-Giemsa staining.

**Bisulfite sequencing**

DNA methylation analysis was performed as described previously[2]. Briefly, genomic DNA was isolated from cells using QIAamp DNA Mini Kit (Qiagen, Hilden, Germany), and bisulfite treatment was performed using the MethylEasy Xceed Kit (Human Genetic Signatures, Sydney, Australia). Modified DNA was amplified by PCR and cloned into a pGEM-T Easy Vector System (Promega, Madison, WI). The bisulfite sequencing-specific primers are listed in Supplementary Table 1. The independent colonies were amplified with the Illustra TempliPhi Amplification kit (GE Healthcare) or NucleoSpin Plasmid EasyPure kit (Macherey-Nagel, Düren, Germany), and then sequenced.

**Chromatin immunoprecipitation (ChIP)**

ChIP was performed as described previously[3]. Briefly, after crosslinking with 0.5% paraformaldehyde for 10 min and quenching with 100 mM glycine for 10 min, cells were lysed and incubated in lysis buffer (50 mM HEPES pH 7.9, 140 mM NaCl, 1mM EDTA pH 8.0, 10% glycerol, 0.5% NP-40, 0.25% TritonX-10) on ice for 10 min. After intensive washes, the pellets were resuspended in shearing buffer (0.1% SDS, 1 mM EDTA pH 8.0, 10 mM

Tris-HCl pH 8.0) and sonicated using S220 ultrasonicators (Covaris, Woburn, MA). For precipitation, anti-H3K27ac (39133; Active Motif, Carlsbad, CA), anti-GFI1 (sc-376949; Santa Cruz Biotechnology), anti-GFI1B (sc-28356X; Santa Cruz Biotechnology), anti-CEBPA (sc-61X; Santa Cruz Biotechnology), anti-TAL1 (ab155195; Abcam, Cambridge, UK), anti-GATA1 (ab11852; Abcam), anti-RUNX1 (ab23980; Abcam), anti- ERG (ab133264; Abcam), anti-LSD1 (ab17721; Abcam), anti-CoREST (ab32631; Abcam), anti-HDAC1 (ab7028; Abcam) or anti-HDAC2 (ab7029; Abcam), and Dynabeads Protein G (Thermo Fisher Scientific) were used. After reverse crosslinking, ChIP DNA was purified with a MinElute PCR Purification kit (Qiagen) and analyzed by quantitative PCR.

**Supplementary Figure 1**

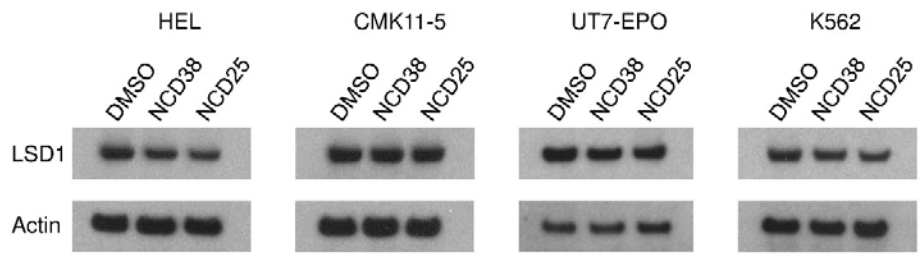


**Supplementary Figure 1**

**LSD1 expression levels in erythro-megakaryocytic leukemia cell lines after exposure to NCD38 or NCD25**

Western blot analysis for the protein expression level of LSD1 after 48-hour treatment with 2 μM NCD38, 2 μM NCD25, or DMSO. Actin was used as a control. Experiments were performed independently twice and representative data are shown.

**Supplementary Figure 2**

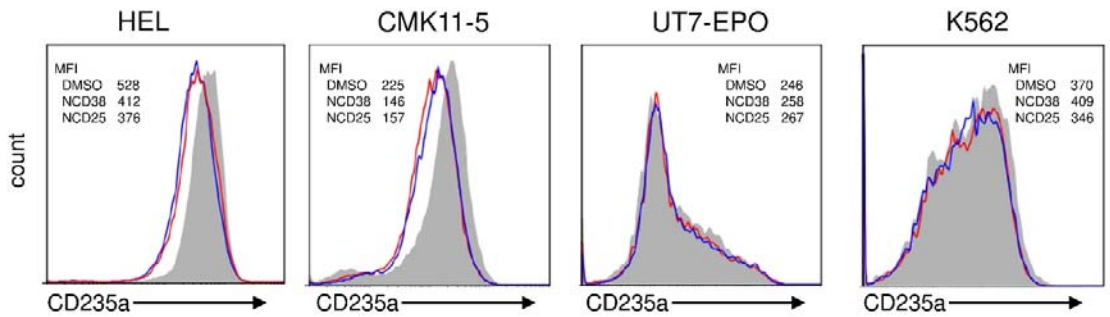


**Supplementary Figure 2**

**Expression change of an erythroid marker, CD235a, in erythro-megakaryocytic leukemia cell lines after exposure to NCD38 or NCD25**

FACS analysis of CD235a in HEL, CMK11-5, UT7-EPO and K562 cells after 48-hour treatment with 2 μM NCD38, 2 μM NCD25, or DMSO. The mean fluorescence intensity (MFI) is presented. Experiments were performed independently three times and representative data are shown.

**Supplementary Figure 3**

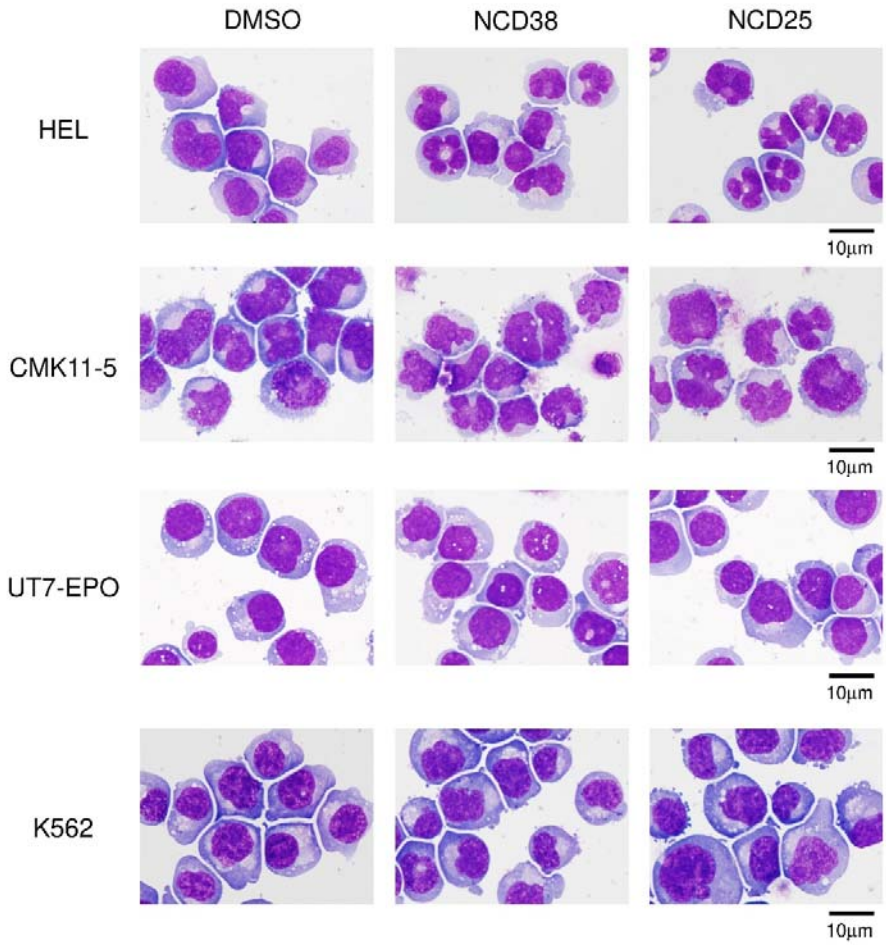


**Supplementary Figure 3**

**Cytological changes in erythro-megakaryocytic leukemia cell lines after exposure to NCD38 or NCD25**

Morphology of HEL, CMK11-5, UT7-EPO and K562 cells after 48-hour treatment with 2 μM NCD38, NCD25 or DMSO. Cytospin slides were stained with traditional Wright-Giemsa staining. Representative pictures are shown. Scale bar indicates 10 μm.

**Supplementary Figure 4**

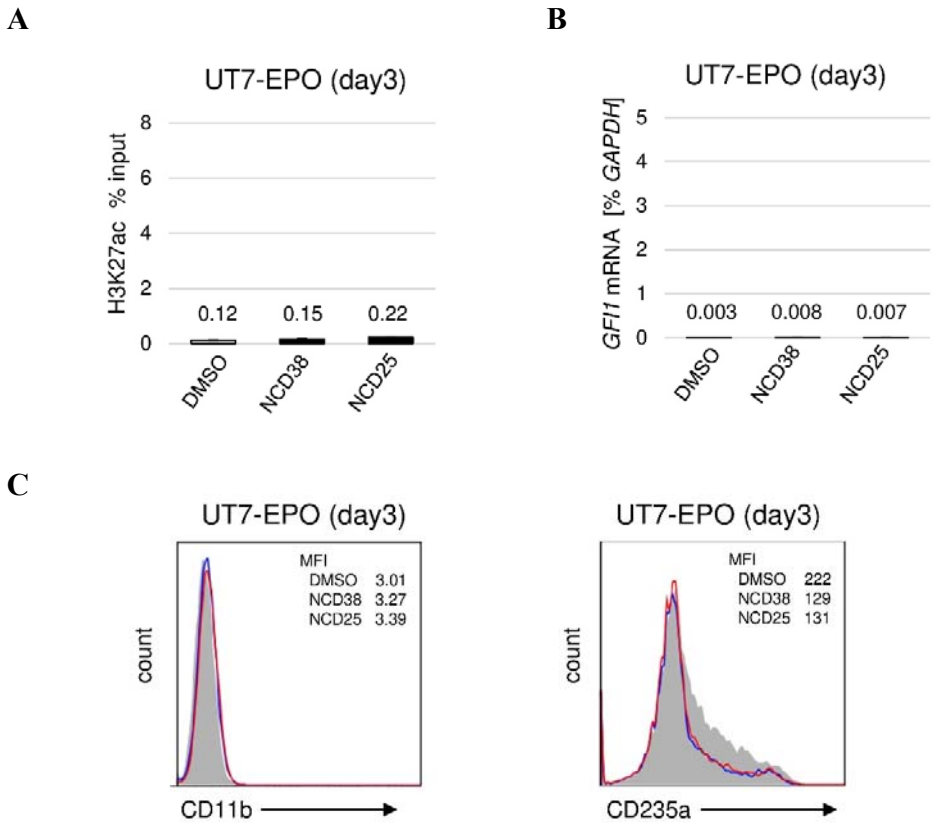


**Supplementary Figure 4**

**H3K27ac in *GFI1*-SE, GFI1 transcript, and cell surface markers CD11b and CD235a in UT7-EPO cells after 72-hour treatment with NCD25 or NCD38**

(a) ChIP-qPCR analysis of H3K27ac in *GFI1*-SE, (b) quantitative PCR analysis of the *GFI1* mRNA level and (c) FACS analysis of CD11b and CD235a in UT7-EPO cells after 72-hour treatment with 2 μM NCD38, 2 μM NCD25, or DMSO. The Y-axes in (a) and (b) indicate

the % input of H3K27ac and the % GAPDH, respectively. The mean fluorescence intensity (MFI) is presented in (c). All experiments were performed independently three times. The means (±SD) are shown in (a) and (b), and representative data are shown in (c).

**Supplementary Figure 5**

**A**

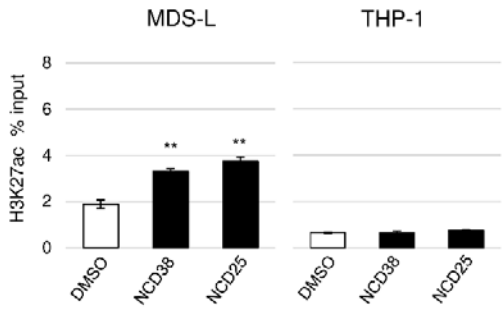


**B**

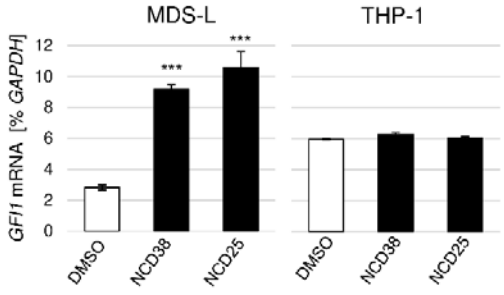


**Supplementary Figure 5**

***GFI1*-SE activation and *GFI1* expression status in MDS-L and THP-1 cells after exposure to NCD38 or NCD25**

(a) ChIP-qPCR analysis of H3K27ac in *GFI1*-SE and (b) quantitative PCR analysis of the *GFI1* mRNA level in MDS-L and THP-1 cells after 48-hour treatment with 2 μM NCD38, 2 μM NCD25, or DMSO. The Y-axes in (a) and (b) indicate the % input of H3K27ac and the % GAPDH. All experiments were performed independently three times and the means (±SD) are shown. *$p < 0.05$, **$p < 0.01$ and ***$p < 0.001$.

**Supplementary Figure 6**

**A.**

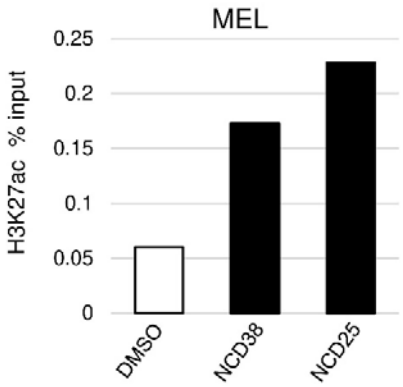


**B.**

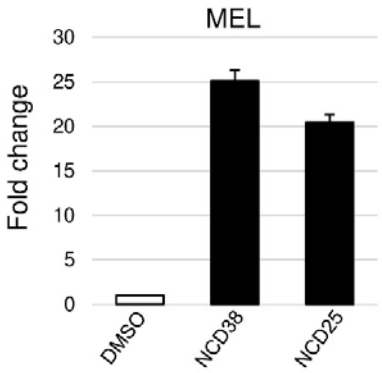


**C.**

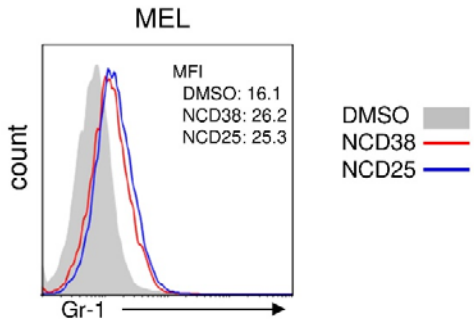


**Supplementary Figure 6**

**Correlation of CA re-activation with myeloid differentiation in murine erythroleukemia**

**(MEL) cells**

(a) ChIP-qPCR analysis of H3K27ac in the CA portion, (b) quantitative PCR analysis of the *Gfi1* mRNA level and (c) FACS analysis of Gr-1 in MEL cells after 48-hour treatment with LSD1 inhibitors including 2 μM NCD38 and 2 μM NCD25, or DMSO as a control. The Y-axes in (a) and (b) indicate % input of H3K27ac and the relative ratio of *Gfi1* mRNA in NCD38 or NCD25 to that in DMSO after normalization by the internal control *Gapdh* mRNA. Mean fluorescence intensity (MFI) is presented in (c). ChIP-qPCR and FACS experiments were performed independently twice. Quantitative PCR experiments were performed independently three times. The means (± SD) are shown in (a) and (b), and representative data are shown in (c).

**Supplementary Figure 7**

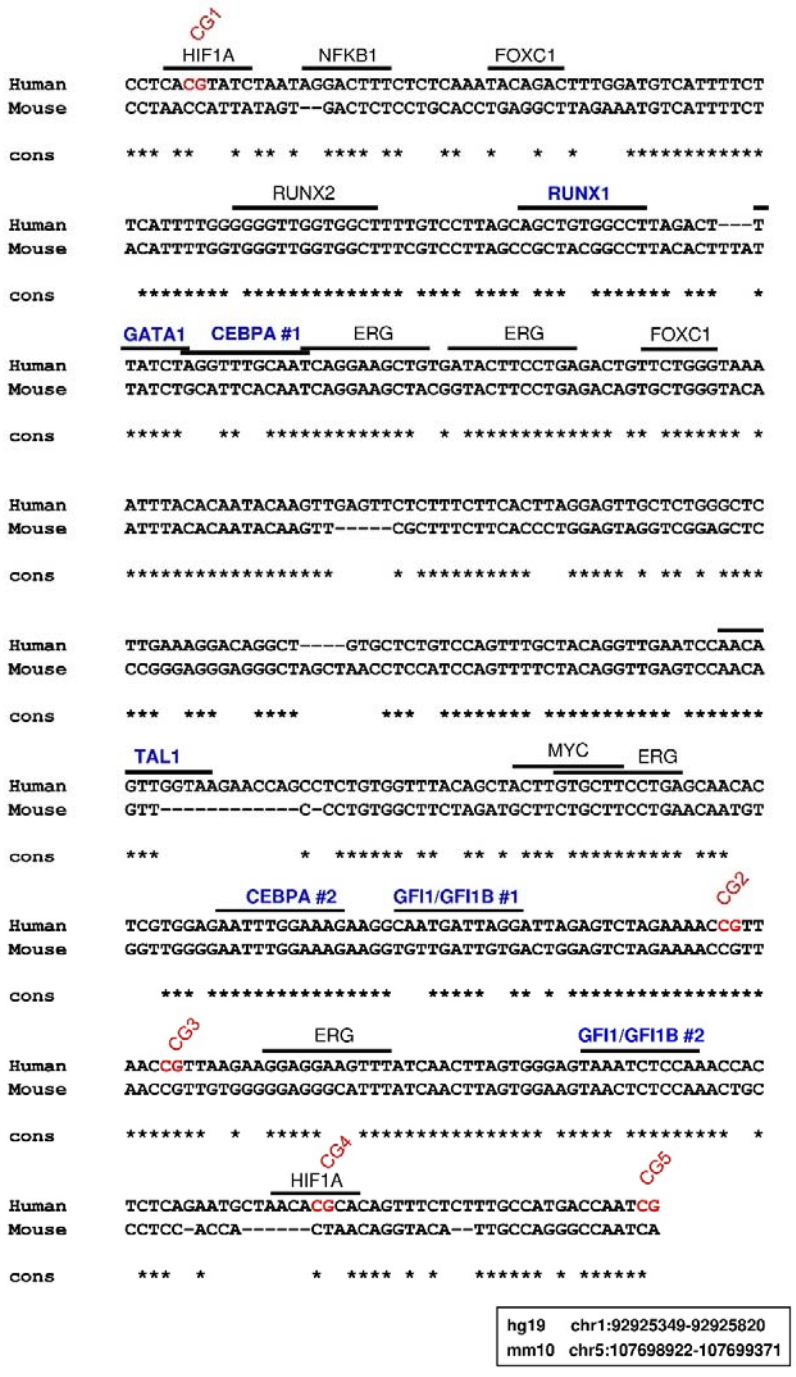


**Supplementary Figure 7**

**TF motifs and CpG sites in the CA of *GFI1*-SE**

Nucleotide sequence alignment between human and mouse of the CA of *GFI1*-SE. The lines above the sequences indicate the TF binding motifs that are related to myeloid differentiation. Several TF binding motifs presented in blue letters are the targets of mutagenesis in the luciferase assay (Fig. 2b). Five CpG sites in the CA of *GFI1*-SE are highlighted in red and each CpG site is numbered. The asterisks indicate the conserved nucleotides.

**Supplementary Figure 8**

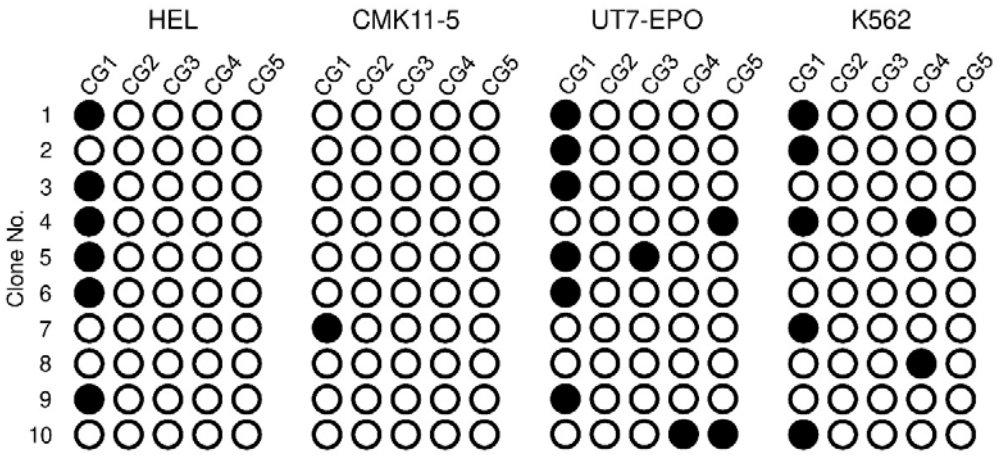


**Supplementary Figure 8**

**DNA methylation status in the CA of *GFI1*-SE in erythro-megakaryocytic leukemia cell lines**

CpG methylation status by bisulfite sequencing in the CA of *GFI1*-SE. Transverse rows and vertical lines represent each single clone and each CpG site, respectively. Solid and open circles indicate methylated and unmethylated CG sites, respectively. Five CpG sites in the CA of *GFI1*-SE are indicated in Supplementary Figure 7.

**Supplementary Figure 9**

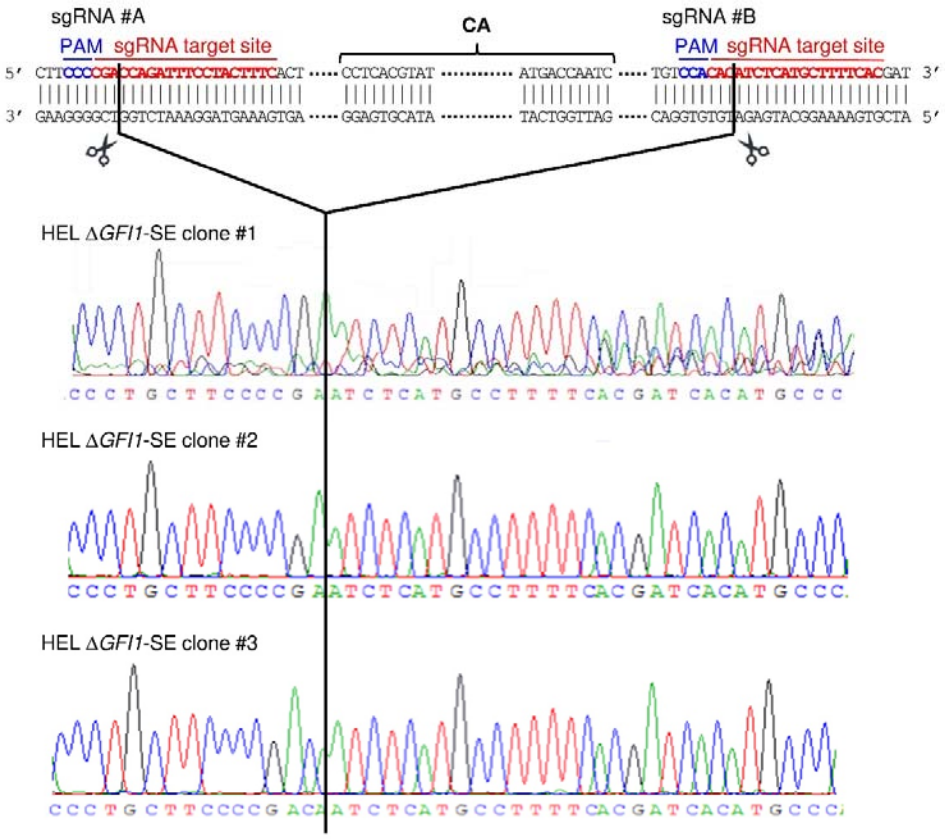


**Supplementary Figure 9**

**Generation of Δ*GFI1*-SE HEL cells by CRISPR-Cas9**

Establishment of Δ*GFI1*-SE sublines of HEL cells. The upper part shows a schematic diagram of the establishment of subclones harboring a *GFI1*-SE knockout allele using the CRISPR-Cas9 genome editing system. The vertical lines indicate the predicted Cas9 cleavage between two sgRNA sequences. The lower part shows Sanger-sequencing results

of the targeted region of three Δ*GFI1*-SE sublines (Δ*GFI1*-SE).

**Supplementary Figure 10**

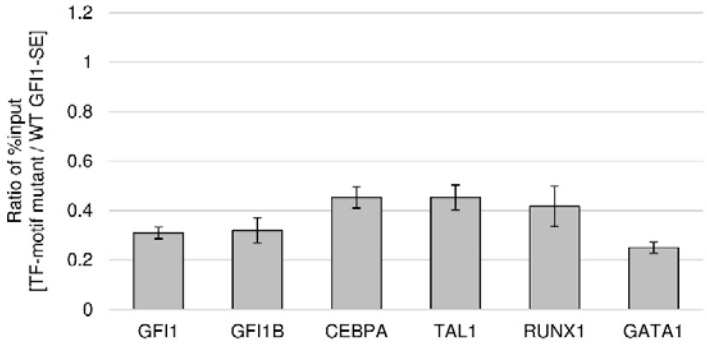


**Supplementary Figure 10**

**Reduction of direct TF recruitment in single TF-motif mutated *GFI1*-SE in Δ*GFI1*-SE cells**

ChIP-qPCR analysis for GFI1, GFI1B, CEBPA, TAL1, RUNX1, and GATA1 after reinduction of each single TF-motif mutant vector or wild-type *GFI1*-SE vector into Δ*GFI1*-SE cells. Data are shown as the ratio of % input of indicated TFs on each TF-motif mutated *GFI1*-SE to that in wild-type *GFI1*-SE. Experiments were performed independently three times and the means (± SD) are shown.

**Supplementary Figure 11**

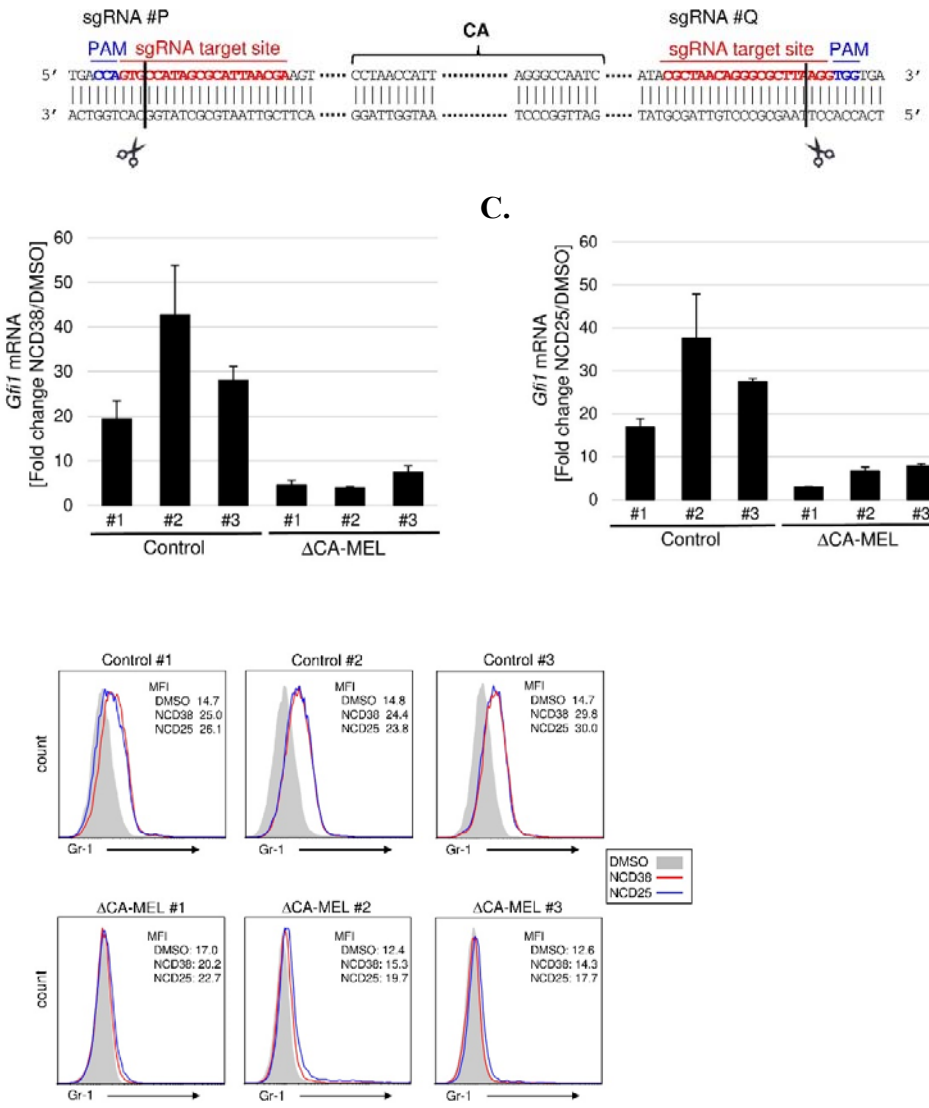


**Supplementary Figure 11**

**Attenuation of myeloid differentiation by NCD38 and NCD25 in ΔCA murine erythroleukemia (MEL) cells**

(a) Schematic diagram of the establishment of subclones harboring the ΔCA allele (MEL-

ΔCA) using the CRISPR-Cas9 genome editing system. The vertical lines indicate the predicted Cas9 cleavage between two sgRNA sequences. (b, c) Fold change of *Gfi1* mRNA after 48-hour treatment with 2 μM NCD38 and NCD25. The fold change was calculated in each subline by dividing *Gfi1* mRNA level in NCD38 or NCD25 by that in DMSO. Experiments were performed independently three times and the means (± SD) are shown. (d) FACS analysis of Gr-1 (Ly-6G). Histogram shows Gr-1 expression on the cell surface of each subline after 48-hour treatment with 2 μM NCD38, NCD25 or DMSO. The filled histograms indicate DMSO-treated cells. The mean fluorescence intensity (MFI) is shown. The experiments were performed independently twice and representative data are shown.

**Supplementary Figure 12**

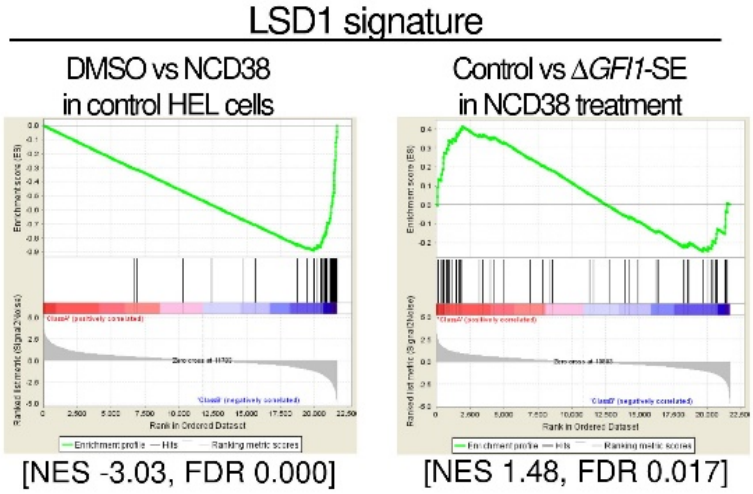


**Supplementary Figure 12**

**GSEA analysis of the LSD1 signature**

The left and right panels present results from comparison between DMSO treatment and NCD38 treatment in control HEL cells and between control HEL cells and Δ*GFI1*-SE HEL cells upon NCD38 treatment, respectively. The normalized enrichment score (NES) and the false discovery rate (FDR) q-value in GSEA are presented at the bottom of each panel. A gene set for the LSD1 signature is listed in Supplementary Table 2.

**Supplementary Figure 13**

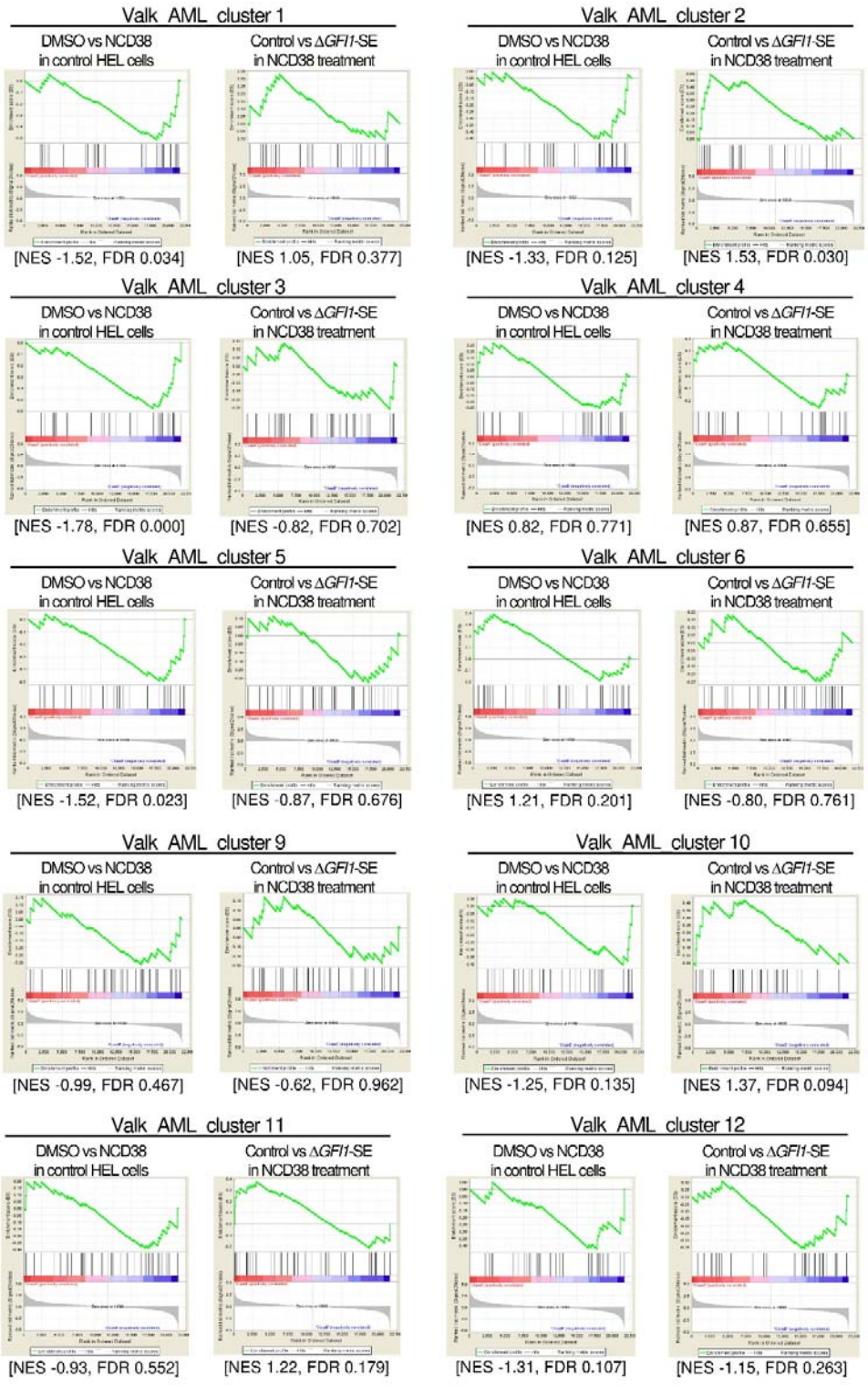

**Supplementary Figure 13, continued**

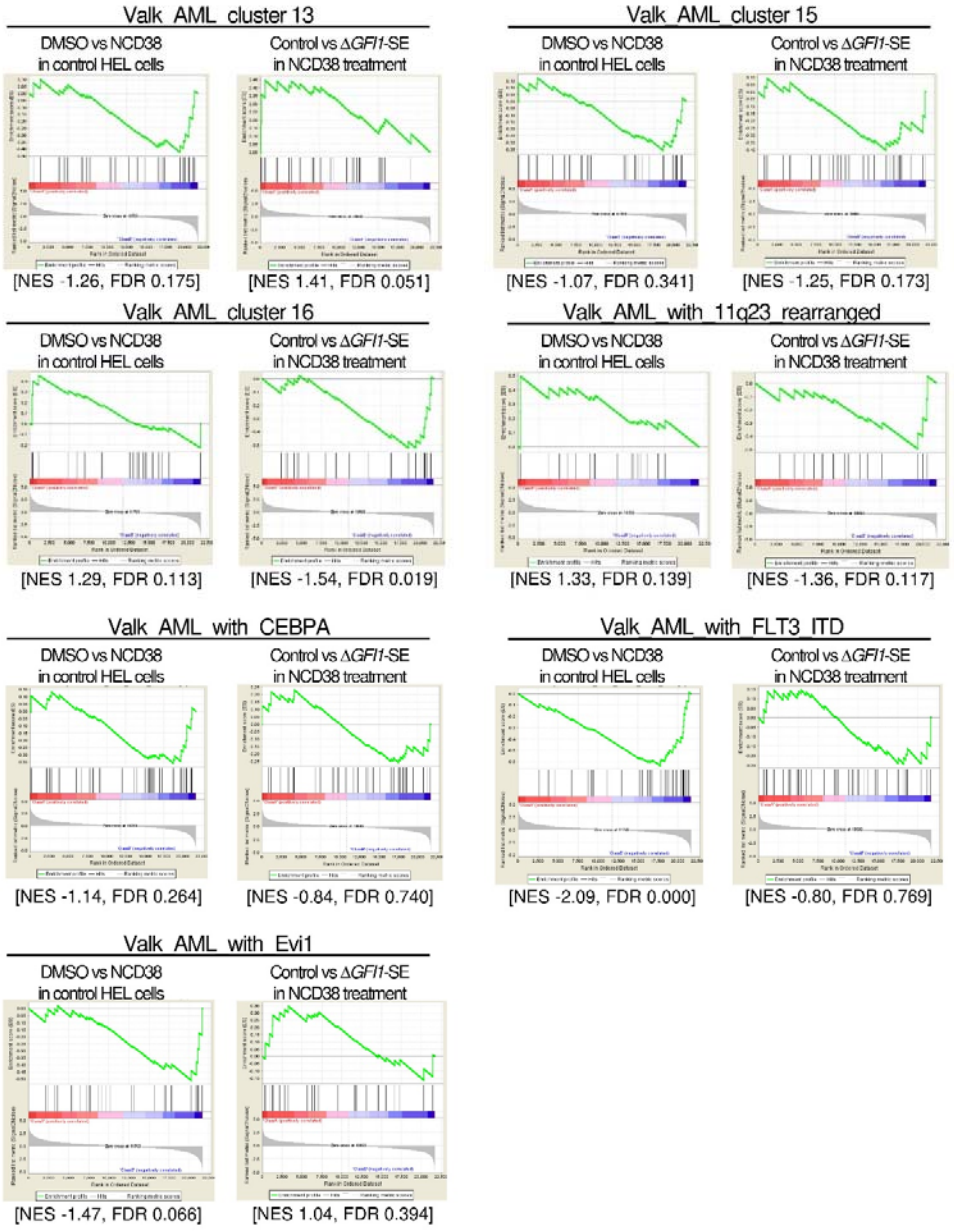

**Supplementary Figure 13**

**GSEA analysis of gene sets of AML from datasets previously reported by Valk et al.**

In each AML cluster signature, the left and right panels present results from the comparison between DMSO treatment and NCD38 treatment in control HEL cells and between control HEL cells and Δ*GFI1*-SE HEL cells upon NCD38 treatment, respectively. The normalized enrichment score (NES) and the false discovery rate (FDR) q-value in GSEA are presented at the bottom of each panel. Gene sets for each AML cluster signature are listed in Supplementary Table 2.

**Supplementary Table 1. Primers and sgRNAs**

Primers for RT-PCR

| | | |
|---|---|---|
| human *GFI1* | Forward | CTCGGAGTTTGAGGACTTCTG |
| | Reverse | CCGCTCCATGAGTACGGTTTG |
| human *GAPDH* | Forward | GAAGGTGAAGGTCGGAGTC |
| | Reverse | GAAGATGGTGATGGGATTTC |
| murine *Gfi1* | Forward | CTATCCCTGTCAGTACTGTGGC |
| | Reverse | CTTGAAGCCTGTGTGCTTTCTG |
| murine *Gapdh* | Forward | AGGTCGGTGTGTGAACGGATTTG |
| | Reverse | TGTAGACCATGTAGTTGAGGTCA |

Primers for ChIP-qPCR

| | | |
|---|---|---|
| human *GFI1*-SE | Forward | TGTCATTTTCTTCATTTTGGGGG |
| | Reverse | CCCAGAGCAACTCCTAAGTG |
| murine CA | Forward | CCAGCCTAACTGTCAGAGGTAAA |
| | Reverse | TCCGCTCCCCTATTTTCTAAGAG |

Primers for bisulfite-specific PCR

| | | |
|---|---|---|
| First half part of CA | Forward | TAAAGGTGATTTTTGTTTGTTTGAG |
| | Reverse | ATTCTTACCAACTATTAAATTCAACCTATA |
| Second half part of CA | Forward | TTTATATAATATAAGTTGAGTTTTTTTT |
| | Reverse | AATTAATTTCCTTCAACAACCTAAC |

sgRNAs for enhancer deletion

| | | |
|---|---|---|
| human *GFI1*-SE | sgRNA #A | GAAAGTAGGAAATCTGGTCGGGG |
| | sgRNA #B | GTGAAAAGGCATGAGATGTGTGG |
| murine CA | sgRNA #P | TCGTTAATGCGCTATGGCACTGG |
| | sgRNA #Q | CGCTAACAGGGCGCTTAAGGTGG |

Genotyping primers for detecting enhancer deletion

| | | |
|---|---|---|
| human *GFI1*-SE | Forward | CCTGATTCTGTGCCTTCTTCATAC |
| | Reverse | GAGTGTGGTTTGACTGTGGTATC |

| | | |
|---|---|---|
| murine CA | Forward | GAAAAATCTGGCATGTCTGTCCC |
| | Reverse | CGGTTTGATTGTTGACACCTGTT |

Primers for generating vectors for luciferase assays

| | | |
|---|---|---|
| cloning *GFI1*-SE | Forward | TTAGAGGAGGCACTGAAAGCAAG |
| | Reverse | CATACTTGTAAGCCCAGCTACTTG |
| deletion of non-CA | Forward | CTTACCTTGCTTTCAGTGCCTCC |
| | Reverse | ACACCCTCACGTATCTAATAGGAC |
| deletion of CA | Forward | AGTCCTATTAGATACGTGAGGGTG |
| | Reverse | GTTGTTGTTGAGATGGAGTCTTGC |
| GFI1/GF1B motif mutant #1 | Forward | ACTCTAATCCTA**C**TCATTGCCTTCTTTC |
| | Reverse | CTAGAAAACCGTTAAGAAGGAGGAAGTT |
| GFI1/GF1B motif mutant #2 | Forward | AGTGGGAGTAA**C**TCTCCAAACCACTCTC |
| | Reverse | AAGTTGATAAACTTCCTCCTTCTTAACG |
| RUNX1 motif mutant | Forward | CTAAGGCCACAGCTGCTAAGGACAAAAG |
| | Reverse | CTAAGG**GG**ACAGCTGCTAAGGACAAAAG |
| GATA1 motif mutant | Forward | ACTTTATCTAGGTTTGCAATCAGGAAGC |
| | Reverse | ACTTTA**C**CTAGGTTTGCAATCAGGAAGC |
| CEBPA motif mutant #1 | Forward | CTTTATCTAGGTTTGC**CC**TCAGGAAGCTGT |
| | Reverse | TCTAAGGCCACAGCTGCTAAGGACAAAAGC |
| CEBPA motif mutant #2 | Forward | AACACTCGTGGAGAA**GG**TGGAAAGAAGGCA |
| | Reverse | GCTCAGGAAGCACAAGTAGCTGTAAACCAC |
| TAL1 motif mutant | Forward | AGGTTGAATCCAA**G**AGTT**T**GTAAGAACCAG |
| | Reverse | GTAGCAAACTGGACAGAGCACAGCCTGTCC |

* The mutation in each motif site is underlined.

**Supplementary Table 2. Gene sets for GSEA analysis**

## A. REGULATION_OF_GRANULOCYTE_DIFFERENTIATION

| | | | | | | |
|---|---|---|---|---|---|---|
| ADIPOQ | C1QC | CUL4A | HAX1 | HCLS1 | IL5 | INPP5D |
| LEF1 | MLL5 | OGT | PRDM16 | RARA | RUNX1 | TESC |
| TRIB1 | ZBTB46 | | | | | |

## B. KAMIKUBO_MYELOID_CEBPA_NETWORK

| | | | | | | |
|---|---|---|---|---|---|---|
| ALDH2 | ANXA1 | CAMP | CASD1 | CD177 | CEBPA | CSF2RA |
| CYBB | DGAT2 | EMR1 | GLRX | HDC | HP | IL18 |
| IRF8 | ITGAM | LBP | LCN2 | LGALS1 | LTF | MMP8 |
| PGD | PRTN3 | RAB31 | S100A8 | S100A9 | SERPINB1 | SPINT2 |

## C. Differentially expressed genes found during erythroid development

| | | | | | | |
|---|---|---|---|---|---|---|
| ALAS2 | ANK1 | ARPC1B | ATP5G1 | BDNFOS | BTG1 | C11orf17 |
| C19orf48 | C19orf6 | C1QBP | CA1 | CAPG | CCDC114 | CCL18 |
| CCL2 | CCL5 | CCT6A | CD44 | CECR1 | CSTB | CTSH |
| CYBA | CYBASC3 | CYP27A1 | EGR1 | ERAF | EYA3 | FADS2 |
| FCGRT | FCN1 | FKBP5 | GDF15 | GIPC1 | GYPC | H3F3A |
| HBA1 | HBB | HBG1 | HBM | HLA-DQA1 | HLA-DRA | HMGN1 |
| IGHG1 | IL8 | ILF3 | ITLN1 | KCNH2 | KHSRP | KIAA1727 |
| LIPA | LOC388588 | LOC399761 | LOC730200 | LXN | LYZ | MGC4677 |
| MMP9 | NDUFA3 | NOP5/NOP58 | NUDT4 | PLA2G7 | PRG1 | PRSS1 |
| PSAP | PSMA2 | REXO2 | RHAG | RNASE1 | RPL22L1 | SELENBP1 |
| SLC12A9 | SLC25A37 | SNHG5 | SOD2 | STK11 | TINP1 | TPSAB1 |
| TRIB3 | TSPAN17 | TYMS | UBE2D3 | UQCRQ | VAV2 | WDR36 |

## D. WELCH_GATA1_TARGETS

| | | | | | | |
|---|---|---|---|---|---|---|
| ABCB10 | ALAD | ALAS2 | ANK1 | BACH1 | EPB49 | FTL |

| | | | | | | |
|---|---|---|---|---|---|---|
| GSTT2 | HBZ | HEBP1 | HMBS | KLF1 | MAFG | MAFK |
| NFE2 | PPOX | SLC4A1 | STOM | TFRC | UROD | UROS |
| ZFPM1 | | | | | | |

**E. Valk_AML_cluster_7**

| | | | | | | |
|---|---|---|---|---|---|---|
| ANK1 | C5ORF4 | CLCN3 | DNAJC6 | EPB41 | GAPVD1 | GDF15 |
| GYPE | HBBP1 | HBZ | KCNH2 | KEL | MYL4 | OSBP2 |
| PDZK1IP1 | RAP1GAP | RHAG | RHD | SELENBP1 | SLC25A37 | SLC2A1 |
| SLC6A8 | SLC6A9 | SPTB | TAL1 | TNS1 | TPM1 | TRIM10 |

**F. Valk_AML_cluster_8**

| | | | | | | |
|---|---|---|---|---|---|---|
| ABCG2 | ANK1 | ARHGEF12 | BCAM | C5ORF4 | CDC42BPA | CDH1 |
| DCAF11 | FECH | GYPA | GYPB | MOSPD1 | MXI1 | OPTN |
| OSBP2 | PBX1 | RHCE | RHD | SELENBP1 | SLC6A8 | SNCA |
| TAL1 | TMEM158 | TNS1 | TRAK2 | TSPAN5 | | |

**G. LSD1 signature**

| | | | | | | |
|---|---|---|---|---|---|---|
| ACVRL1 | ARHGEF11 | BST2 | CALHM2 | CCR2 | CCSER2 | CLEC4A |
| CNR2 | CORO2A | CTSV | EFNA4 | ERG | FCGR1B | FCGR2B |
| FCRLA | FOSL2 | GCNT1 | GFI1 | GFI1B | HLA-DMB | HVCN1 |
| HYLS1 | IL18R1 | IL18RAP | IL4I1 | ISY1-RAB43 | KIAA0513 | LAIR1 |
| LMO4 | LOC388242 | LPXN | METTL7A | MILR1 | OIT3 | OSBPL11 |
| P2RY14 | PI16 | PIK3C2B | PLD2 | PNRC1 | PPP1R13B | PROCR |
| PRR9 | RAB43 | RASSF4 | S1PR1 | SELL | SIDT2 | SIGLEC17P |
| SLC35F6 | SLC7A8 | SNX21 | SPTAN1 | STAB1 | TIGD3 | TLR1 |
| TMEM243 | TNFRSF10D | TNFSF10 | TPM4 | TRAF5 | ZBTB46 | |

**H. Valk_AML_cluster_1**

| | | | | | | |
|---|---|---|---|---|---|---|
| ATF3 | ATP10A | BHLHE41 | BLNK | BMI1 | COBLL1 | DPP4 |

| | | | | | | |
|---|---|---|---|---|---|---|
| FHL1 | GPR126 | IGHM | IRF7 | JUN | KCNA5 | KIF17 |
| LTBP3 | MECOM | MEF2C | MMRN1 | NR4A2 | PCDH9 | PROM1 |
| PRR16 | SLC2A3 | SLC38A1 | SOCS2 | SPAG6 | SPIB | TRPS1 |

## I. Valk_AML_cluster_2

| | | | | | | |
|---|---|---|---|---|---|---|
| ARHGAP22 | CCL1 | CLU | DOCK1 | EZR | GLI2 | GOLGA8A |
| GOLGA8B | GPR56 | GRB10 | GUCY1A3 | HBB | HOXA5 | HOXB2 |
| IL2RA | JAG1 | KCNK5 | LAPTM4B | LPIN1 | MAP4K4 | PDE3B |
| PIM1 | PLA2G4A | PLS1 | PTP4A3 | SCHIP1 | SRSF8 | TRIM16 |
| TRPC2 | | | | | | |

## J. Valk_AML_cluster_3

| | | | | | | |
|---|---|---|---|---|---|---|
| ADCY2 | AGTPBP1 | AIM1 | ARHGAP22 | BLVRA | CCL1 | CEBPD |
| COL4A5 | DOCK1 | ENPP4 | FAM30A | FCGRT | GAS2 | GPR56 |
| IL17RA | IL6ST | LAPTM4B | MAP7 | NET1 | PBXIP1 | PDGFD |
| PIEZO2 | PLS1 | QPRT | RAP2A | SCN9A | SEPP1 | SERPINB8 |
| SH2D1A | SMC4 | TNFRSF4 | TRIM16 | WBP5 | | |

## K. Valk_AML_cluster_4

| | | | | | | |
|---|---|---|---|---|---|---|
| ABCB1 | B4GALT6 | C18ORF1 | CAPN2 | CD7 | CFD | CSDA |
| CTNNA1 | CYFIP1 | DRAM1 | FZD6 | HPGDS | HPS4 | IGFBP7 |
| IKZF2 | IL4R | ITGA4 | KLF2 | LRP10 | NDFIP1 | P2RX5 |
| PMS2L2 | PMS2P3 | PRR5L | RAB13 | TRAT1 | TRDV2 | TRIB1 |
| TSPAN7 | TUBB6 | UGT2B28 | | | | |

## L. Valk_AML_cluster_5

| | | | | | | |
|---|---|---|---|---|---|---|
| CAMK1 | CCR1 | CD86 | EFHD2 | EPB41L3 | FAM198B | GNS |
| HNMT | IFNGR2 | KCNQ1 | LILRA1 | LILRA6 | LILRB1 | LILRB2 |
| LILRB3 | MAFB | NOD2 | PILRA | PSAP | PTAFR | RASSF4 |

| | | | | | | |
|---|---|---|---|---|---|---|
| SIGLEC7 | SIRPA | SIRPB1 | SLC15A3 | SMPDL3A | STS | TFEB |
| TLR8 | TYMP | UBE2D1 | VCAN | VDR | | |

## M. Valk_AML_cluster_6

| | | | | | | |
|---|---|---|---|---|---|---|
| ADCY2 | BST2 | CAT | CD74 | CEP70 | CORO1A | DPPA4 |
| DPYSL3 | DSC2 | FAM110B | FAM174B | FOXC1 | FOXF2 | FTO |
| GPC4 | HIGD1A | HLA-DPA1 | HLA-DRA | HOXB3 | KIAA0930 | LTBP1 |
| NT5DC3 | PECAM1 | PIEZO2 | PLXNB1 | RGS10 | RSL1D1 | SLC27A6 |
| SMC4 | SNCAIP | TTC27 | TUBGCP4 | XPA | | |

## N. Valk_AML_cluster_9

| | | | | | | |
|---|---|---|---|---|---|---|
| AK5 | BAHCC1 | CBFB | CD1C | CD59 | CD81 | CHI3L1 |
| CHST12 | CLEC10A | CLIP2 | CLIP3 | COLEC12 | DHRS3 | EMID1 |
| FAM105A | FAM171A1 | FCGR2B | ICAM4 | MGLL | MN1 | MSLN |
| MTMR11 | MYH11 | NDE1 | NRP1 | NT5E | PAPSS2 | PTPRM |
| RPS6KA2 | RUNX3 | SPARC | ST18 | TGFBI | TPPP3 | VSIG4 |

## O. Valk_AML_cluster_10

| | | | | | | |
|---|---|---|---|---|---|---|
| ARHGEF17 | AZU1 | BAALC | BCL7A | C3AR1 | CD22 | CFD |
| CHRDL1 | CRIM1 | EEF1A2 | F2RL1 | FAM30A | FLNB | GNAI1 |
| IGHM | LPHN1 | MLLT3 | MN1 | NPDC1 | PAWR | PIK3C2B |
| PPP1R16B | PRKD2 | RBPMS | RNASE2 | SETBP1 | SMAGP | SNED1 |
| SORBS3 | SPON1 | SPRY1 | SPTBN1 | TPM2 | | |

## P. Valk_AML_cluster_11

| | | | | | | |
|---|---|---|---|---|---|---|
| ALDH2 | APP | ASS1 | CD200 | CD34 | CIITA | CISH |
| CLIC4 | DAB2 | DAPK1 | DNM1 | DPYSL2 | DUSP7 | EGFL7 |
| EVL | FYN | GAS2L1 | GIMAP5 | GIMAP6 | H1F0 | IFITM1 |
| ITGA6 | KCNN4 | KLF9 | KYNU | LHFPL2 | LPAR6 | MDFIC |

| | | | | | | |
|---|---|---|---|---|---|---|
| MYO5C | PALM | REEP5 | SERPINB9 | SLC38A1 | SPARC | ST3GAL5 |
| VEGFA | | | | | | |

## Q. Valk_AML_cluster_12

| | | | | | | |
|---|---|---|---|---|---|---|
| AFF2 | ALADL1 | ARHGAP4 | AZI2 | CALR | CST7 | FGF13 |
| GABRE | GALNT3 | HGF | LAMC1 | LGALS9 | MEG3 | MFNG |
| MST1 | MXRA7 | NKX3-2 | NRIP1 | P4HB | PCBP3 | PRODH |
| PTCH1 | PTGDS | PTGER1 | RAB5B | SIX3 | SKAP2 | STXBP1 |
| TMEM87A | VCL | | | | | |

## R. Valk_AML_cluster_13

| | | | | | | |
|---|---|---|---|---|---|---|
| ADCY7 | ADRA2C | BAIAP3 | C11ORF21 | C11ORF9 | C15ORF39 | CACNA2D2 |
| CAV1 | FBLN5 | GRK5 | HSPG2 | IL5RA | ITGB4 | KDM4B |
| LAT2 | LCP1 | NBL1 | NCALD | PNMT | POU4F1 | PSD3 |
| RFL | ROBO1 | RUNX1T1 | SLC25A1 | STK32B | THSD7A | TRH |
| VLDLR | VOPP1 | | | | | |

## S. Valk_AML_cluster_15

| | | | | | | |
|---|---|---|---|---|---|---|
| ARHGEF3 | ATN1 | BASP1 | CD52 | CEACAM8 | CTNNA1 | DRAM1 |
| ECHDC2 | EPB41L2 | FADS1 | GNA12 | GRAMD1B | HOXA10 | HOXA9 |
| HOXB2 | HOXB5 | HSPB1 | IGF2BP2 | IGHM | KLF9 | MEIS1 |
| NDFIP1 | RUNX1 | SEL1L3 | SFXN3 | SH3TC1 | SLC16A1 | SUCLG2 |
| TBL1X | TNS3 | TUBB6 | | | | |

## T. Valk_AML_cluster_16

| | | | | | | |
|---|---|---|---|---|---|---|
| ADCY9 | AK2 | AKR7A2 | APOC2 | BRE | C1ORF54 | C20ORF103 |
| C3ORF14 | CACNA2D3 | CADM1 | CD70 | CLSTN2 | DACH1 | GGA2 |
| ITGA7 | KCNE1L | KCNN2 | MBNL1 | PENK | RET | RPP25 |
| TDRD7 | TGM5 | TKTL1 | TRPM4 | UVRAG | | |

## U. Valk_AML_with_11q23_rearranged

| | | | | | | |
|---|---|---|---|---|---|---|
| APOC2 | C1ORF54 | C20ORF103 | C3ORF14 | CACNA2D3 | CADM1 | CD70 |
| CES1 | DACH1 | HIF1A | ITGA7 | KCNE1L | LOC283683 | MSLN |
| NXT2 | P2RY2 | PENK | RET | TGM5 | TKTL1 | TRPM4 |
| UVRAG | | | | | | |

## V. Valk_AML_with_CEBPA

| | | | | | | |
|---|---|---|---|---|---|---|
| ARHGEF3 | ATN1 | B4GALT6 | BASP1 | CAMP | CD38 | CD7 |
| CEACAM8 | CEBPA | CTNNA1 | DLC1 | GALC | GNA12 | HOXA9 |
| HOXB2 | HPGDS | HSPB1 | IGF2BP2 | IGHM | IGLL1 | ITM2A |
| LCN2 | LTF | MEST | MMP8 | NDFIP1 | PGLYRP1 | PRR5L |
| SEL1L3 | SFXN3 | SLC16A1 | SUCLG2 | TBL1X | TNS3 | TRDV2 |
| TRIB1 | TUBB6 | | | | | |

## W. Valk_AML_with_FLT3_ITD

| | | | | | | |
|---|---|---|---|---|---|---|
| ADCY2 | APP | BAHCC1 | COL4A5 | CYSLTR2 | ENPP2 | GOLGA8A |
| GOLGA8B | GPR56 | HOXA4 | HOXA5 | HOXA9 | HOXB2 | HOXB3 |
| HOXB5 | HOXB6 | IL1RAP | IL2RA | KCNK5 | LAPTM4B | LCT |
| LGALS3BP | LYRM1 | MAGED1 | MAP1A | MMP2 | MRC1 | NR6A1 |
| PBX3 | PDE4B | PDGFD | PIEZO2 | PIM1 | QPRT | SEPP1 |
| SMC4 | SOCS2 | TARP | TRIM16 | TRPC2 | | |

## X. Valk_AML_with_EVI1

| | | | | | | |
|---|---|---|---|---|---|---|
| AZU1 | CD34 | CFD | CRIM1 | DMXL2 | EEF1A2 | F2RL1 |
| FAM30A | GNAI1 | IGHM | LPHN1 | MN1 | NPDC1 | PAWR |
| PIK3C2B | PPP1R16B | PXDN | RBPMS | RNASE2 | RNASE3 | SEPX1 |
| SMAGP | SORBS3 | SPRY1 | SPTBN1 | | | |

**Supplementary Table 3. List of genes influenced by *GFI1*-SE depletion**

Genes that were induced more than two-fold by NCD 38 but whose inductions were attenuated by less than 50% via *GFI1*-SE depletion

| Gene Symbol | Fold Change [DMSO vs NCD38 in control HEL cells] | Fold Change [Control vs ΔGFI1-SE in NCD38 treatment] | Fold Change [DMSO vs NCD38 in CMK11-5 cells (Dataset: GSE68348)][4] |
|---|---|---|---|
| LOC101928012 | 12.35 | 5.50 | 13.43 |
| PRR9 | 10.62 | 4.44 | 7.00 |
| GFI1 | 8.05 | 2.85 | 9.07 |
| S1PR1 | 6.27 | 2.59 | 7.39 |
| SLC45A3 | 6.24 | 3.08 | 3.17 |
| TEK | 5.33 | 2.28 | 3.24 |
| TRGJP2 | 4.37 | 1.32 | 2.41 |
| STYK1 | 3.56 | 1.56 | 2.73 |
| ERG | 3.54 | 1.76 | 4.58 |
| CD200R1 | 2.69 | 1.22 | 7.98 |
| RP11-702L15.4 | 2.36 | 1.18 | NA |
| IGFBP4 | 2.08 | 0.96 | 2.47 |
| RNU6-795P | 2.07 | 0.83 | NA |
| MIR296 | 2.06 | 0.71 | NA |
| RP11-758M4.4 | 2.05 | 0.92 | NA |
| RP11-661A12.4 | 2.02 | 0.91 | NA |
| RPL23AP32 | 2.00 | 0.93 | 1.99 |

Genes that were attenuated by less than 50% by NCD 38 but whose reductions were recovered more than two-fold via *GFI1*-SE depletion

| Gene Symbol | Fold Change [DMSO vs NCD38 in control HEL cells] | Fold Change [Control vs ΔGFI1-SE in NCD38 treatment] | Fold Change [DMSO vs NCD38 in CMK11-5 cells (Dataset: GSE68348)][4] |
|---|---|---|---|
| THBS1 | 0.41 | 1.07 | 0.33 |
| CCR4 | 0.41 | 0.94 | 0.91 |

| | | | |
|---|---|---|---|
| RHD | 0.42 | 0.84 | 0.15 |
| FAM19A3 | 0.46 | 0.93 | 0.45 |
| RNA5SP302 | 0.49 | 1.03 | NA |

NA; not available in this data set (GSE68348) due to differences between the platforms used for separate analyses (Affymetrix vs. Agilent).

**Supplementary References**


1. Tohyama K, Tohyama Y, Nakayama T, Ueda T, Nakamura T, Yoshida Y. A novel factor-dependent human myelodysplastic cell line, MDS92, contains haemopoietic cells of several lineages. *British journal of haematology* 1995 Dec; **91**(4)**:** 795-799.

2. Shimazu Y, Hishizawa M, Hamaguchi M, Nagai Y, Sugino N, Fujii S, *et al.* Hypomethylation of the Treg-Specific Demethylated Region in FOXP3 Is a Hallmark of the Regulatory T-cell Subtype in Adult T-cell Leukemia. *Cancer Immunol Res* 2016 Feb; **4**(2)**:** 136-145.

3. Yamamoto R, Kawahara M, Ito S, Satoh J, Tatsumi G, Hishizawa M, *et al.* Selective dissociation between LSD1 and GFI1B by a LSD1 inhibitor NCD38 induces the activation of ERG super-enhancer in erythroleukemia cells. *Oncotarget* 2018 Apr 20; **9**(30)**:** 21007-21021.

4. Sugino N, Kawahara M, Tatsumi G, Kanai A, Matsui H, Yamamoto R, *et al.* A novel LSD1 inhibitor NCD38 ameliorates MDS-related leukemia with complex karyotype by attenuating leukemia programs via activating super-enhancers. *Leukemia* 2017 Nov; **31**(11)**:** 2303-2314.